Chemical Engineering Journal 162 (2010) 273–277

Contents lists available at ScienceDirect

Chemical Engineering Journal

journal homepage: www.elsevier.com/locate/cej

Kinetic transitions during Ag and Cu electrorecovery on reticulated vitreous carbon electrodes in flow-by mode

Q. de Radiguès, R. Santoro, J. Proost*

Division of Materials and Process Engineering, Université catholique de Louvain, B-1348 Louvain-la-Neuve, Belgium

ARTICLE INFO

Article history:
Received 18 February 2010
Received in revised form 20 May 2010
Accepted 22 May 2010

Keywords:
Porous electrodes
Electrochemical recovery
Kinetics
Filter press cell

ABSTRACT

This paper reports on the kinetics of the galvanostatic electrorecovery of copper and silver from sulphate solutions on a reticulated vitreous carbon cathode in flow-by mode. The influence of applied current and flow rate on the electrorecovery rate was systematically studied. Detailed analysis of the electrorecovery kinetics revealed two regimes. The first one was found to be electron-transfer limited, while the second one appeared to be mass transfer limited. From the relevant kinetic rate constants, a current efficiency of 1.03 ± 0.03 for Ag and 0.88 ± 0.01 for Cu electrorecovery was obtained in the first regime. For the second regime, the characteristic mass transport coefficients were determined as $(7.6 \pm 0.3) \times 10^{-3}$ and $(22.6 \pm 0.03) \times 10^{-3}$ cm/s for Ag and Cu, respectively. Analysis of the time and concentration at the kinetic transition was shown to allow for an additional, independent calculation of both the current efficiency and mass transport coefficient, and to confirm that the kinetic transitions occur when the limiting current has been reached.

© 2010 Elsevier B.V. All rights reserved.

1. Introduction

Environmental concerns nowadays require the removal of metal ions from industrial wastewaters down to the ppm level. The cathodic removal of these ions has been used for several years, as it allows for the recovery of the considered metal in pure form without having to deal with process sludges. The use of porous electrodes allows for the recovery of metal ions to much lower concentrations as compared to conventional two-dimensional electrodes. Reticulated vitreous carbon (RVC) has naturally become a material of great interest in this field due to its low cost, high surface area, chemical inertness, low resistance to fluid flow and good electrical conductivity [1].

Electrodeposition of metal ions on RVC is already a widely discussed area. Agarwal et al. [2] showed the feasibility of electrorecovery of several metal ions on RVC cathodes from acidic sulphate solution, including copper and cadmium. Copper electrorecovery in particular has been widely used as a model system for testing cells with 3D electrodes. Mass transport properties of potentiostatic electrodeposition of copper from acid sulphate solutions have been characterized by Pletcher et al. [3] in a flow-by cell. These authors also discussed the performance of flow-by cells in batch recycle mode [4] and single pass mode [5]. Recent developments on RVC rotating cylinder cathodes have been discussed by Reade et al. [6]. Nikolic et al. [7] observed the formation of dish-like holes in copper electrodeposits on a copper wire under the influence of hydrogen bubbles. Saleh [8] suggested that hydrogen bubbles generated at a porous cathode could enhance the mass transfer locally.

This paper specifically concentrates on the kinetic details of electrodeposition of Cu and Ag on RVC, using a flow-by cell under galvanostatic conditions in batch recycle mode. The choice of the metallic elements was largely motivated by their presence in wastewaters of the plating industry. Contrary to most of the previous work in the field, our experiments have been carried out from effluents with a relatively high initial metal ion concentration, in the order of 1000 mg/L for Ag and 350 mg/L for Cu, in order to see whether the electrorecovery on porous electrodes would still be feasible at such high initial concentrations. By doing so, the systematic study of the influence of applied current and flow rate revealed for the first time two different kinetic regimes. The first one, when the metal ion concentration in the bulk solution is still relatively high, is limited by electron transfer. When the metal concentration in solution gradually decreases, mass transfer becomes limiting. From the kinetic rate constant of the first regime, current efficiencies for Ag and Cu electrorecovery have been determined. The kinetic rate constant of the second regime allowed for calculating the mass transport coefficient characteristic for Ag and Cu electrorecovery. Finally, a detailed analysis of the time and concentration at the kinetic transition was shown to allow for an

* Corresponding author at: Division of Materials and Process Engineering, Université catholique de Louvain, Réaumur Building, Place Sainte-Barbe 2, 1348 Louvain-la-Neuve, Belgium. Tel.: +32 10 47 93 42; fax: +32 10 47 40 28.
E-mail address: joris.proost@uclouvain.be (J. Proost).

1385-8947/$ – see front matter © 2010 Elsevier B.V. All rights reserved.
doi:10.1016/j.cej.2010.05.046

Nomenclature

List of symbols

C_0	initial concentration in the bulk solution (mol m^{-3})
V_e	volume of the electrode (m^3)
A_e	specific surface of the cathode (m^{-1})
C	concentration in the bulk solution (mol m^{-3})
k_1	kinetic rate constant in the first regime (mol m^{-3} s^{-1})
k_2	kinetic rate constant in the second regime (s^{-1})
q	electric charge (C)
t	time (s)
I	applied current (A)
η	current efficiency (−)
z	number of exchanged electrons (−)
F	Faraday constant (A s mol^{-1})
V	volume of the catholyte (m^3)
k_m	mass transfer coefficient (s^{-1})
D	diffusion coefficient (m^2/s)
δ	thickness of the diffusional boundary layer (m)
I_{lim}	limiting current (A)
C_{trans}	concentration in the bulk solution at the transition (mol m^{-3})
v	mean linear flow velocity (m/s)

additional, independent calculation of both the current efficiency and mass transport coefficient.

2. Experimental details

All experiments were carried out at room temperature from 1 L, 0.5 M sulphuric acid catholyte solutions with an initial nominal concentration (C_o) aimed at, respectively, 5 ± 0.5 mM of Cu^{2+} and 10 ± 0.5 mM of Ag^+. The relative concentrations of the two ions in the catholyte were chosen based on charge equivalency. The anolyte was always 0.5 M sulphuric acid. Metal ion concentrations have been analyzed ex situ with a Varian ICP-OES on 10 mL samples taken from the bulk catholyte during each electrorecovery experiment. The three-dimensional cathode, 35 mm × 35 mm × 6 mm in volume (V_e) was cut from 100 ppi reticulated vitreous carbon (RVC) with a specific surface $A_e = 66$ cm^2/cm^3.

Experiments were performed in a commercial electrochemical filter press cell (Micro Flow cell from Electrocell), shown schematically in Fig. 1(a). The two compartments were separated by a Nafion 350 cationic membrane. A piece of RVC was placed in the centre of the cathodic compartment and compressed onto the stainless steel cathode. The electrical contact made by these collectors generated a current flow perpendicular to the electrolyte flow (flow-by configuration). An upstream flow was imposed to avoid gaseous accumulation in the electrode compartments. The electrochemical cell was inserted into a hydraulic circuit, shown schematically in Fig. 1(b). It comprises two pumps forcing the circulation of the electrolyte in each compartment of the filter press cell. The electrolyte then flows back into a 1 L stirred tank. The pumping rate was adjusted in order to obtain an electrolyte flow varying from 0.26 to 1.0 L/min in the catholyte compartment and constant at 1.2 L/min in the anolyte compartment. The corresponding mean linear flow velocities v, defined as the ratio of volumetric flow rate to the electrode cross-sectional area, therefore varied from 1.3×10^{-2} to 8×10^{-2} m/s in the catholyte compartment. The experiments were carried out under galvanostatic conditions, with the applied current ranging from 0.27 to 1.5 A.

3. Results and discussion

3.1. Kinetic rate constants

Fig. 2 shows a typical evolution of the metal concentration with time, represented on both a linear (a) and a normalised logarithmic (b) scale. Two kinetic regimes can clearly be distinguished. In the first regime, the evolution of the concentration was observed to decrease linearly with time (Fig. 2(a)). It thus follows a zero order kinetics of the form:

$$\frac{dC}{dt} = -k_1 \Rightarrow C = -k_1 t + C_o \tag{1}$$

with C the concentration in the bulk solution and k_1 the kinetic rate constant of the first regime. In the second regime, a linear decrease of $\ln(C/C_o)$ with time is observed (Fig. 2(b)). This points to a first order kinetics of the form:

$$\frac{dC}{dt} = -k_2 C \Rightarrow \ln\left(\frac{C}{C_o}\right) = -k_2 t \tag{2}$$

k_2 being the relevant kinetic rate constant for the second regime.

Fig. 3 represents the evolution of the rate constant k_1 with applied current for the 2 metal ions considered. They are seen to increase linearly with current, indicating that the first regime is electron-transfer limited. Indeed, the rate constant for a kinetic regime limited by electron transfer can be rationalised from Faradays' law:

$$q = \eta I t \Rightarrow C = C_o - \frac{\eta I t}{zFV} \Rightarrow k_1 \equiv -\frac{dC}{dt} = \frac{\eta I}{zFV} \tag{3}$$

with q the total amount of charge passed at time t, I the applied current, η the current efficiency for electrorecovery, z the number of exchanged electrons, F Faraday's constant and V the volume of the catholyte solution. From Eq. (3), the slope of a linear fit of k_1 vs. I therefore allows to calculate the current efficiencies η. This results in $\eta = 0.88 \pm 0.01$ for Cu and 1.03 ± 0.03 for Ag, the latter error margin being indicative for a 100% electrorecovery efficiency in the case of Ag. We can also point out that, at fixed current densities, k_1 was found to be independent of flow velocity, with average values of

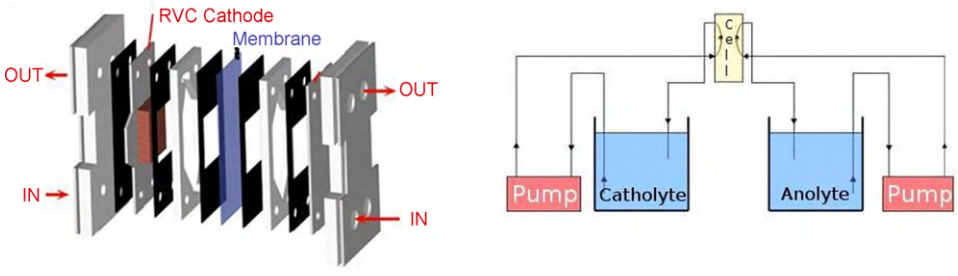

Fig. 1. (a) Schematic of a filter press type electrochemical cell with a porous, three-dimensional cathode, operating in flow-by configuration. (b) Insertion of the cell in the hydraulic circuit.

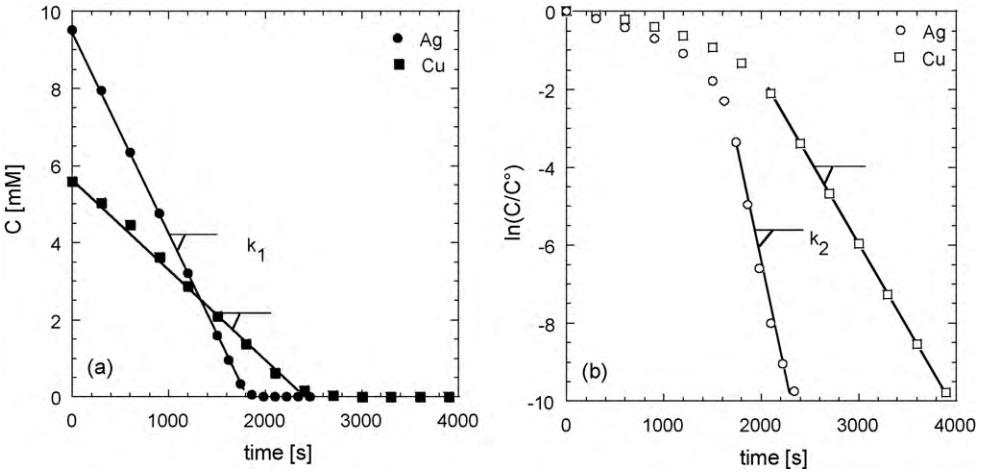

Fig. 2. Evolution of the metal concentration with time on a (a) linear and (b) normalised semi-logarithmic scale ($I = 0.5$ A, $v = 7 \times 10^{-2}$ m/s).

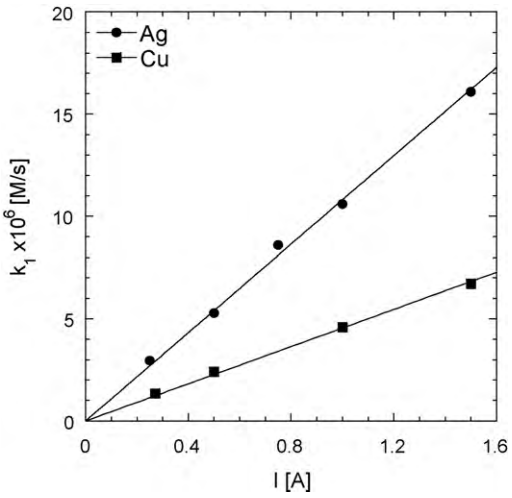

Fig. 3. Evolution of k_1, the kinetic rate constant of the first regime, with applied current ($v = 7 \times 10^{-2}$ m/s).

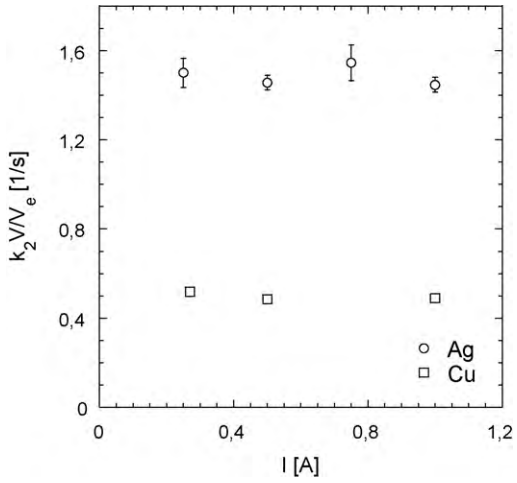

Fig. 4. Evolution with applied current of the kinetic rate constant k_2 of the second regime, normalised by the factor V/V_e ($v = 7 \times 10^{-2}$ m/s).

$5.4 \pm 0.1 \times 10^{-6}$ M/s for Ag ($I = 0.5$ A) and $1.29 \pm 0.02 \times 10^{-6}$ M/s for Cu ($I = 0.27$ A), in agreement with the results of Fig. 3.

Fig. 4 shows the evolution with applied current of the rate constant k_2, normalised by the factor V/V_e, for Cu and Ag electrodeposition, respectively. Fig. 5 shows the same parameter k_2V/V_e as a function of flow velocity v. From Fig. 4, it appears that k_2V/V_e is independent of current density, therefore suggesting that the second regime is not limited by electron transfer. On the other hand, the observed increase with v observed in Fig. 5 suggests that the second regime is rather controlled by mass transfer. The applied normalisation factor in Fig. 5 results from the fact that, as demonstrated in [3], a simple batch reactor approach under mass transfer conditions leads to the following expression for the evolution of the metal ion concentration with time:

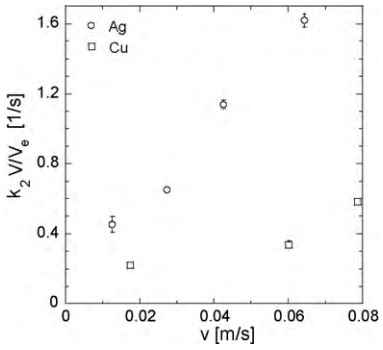

Fig. 5. Evolution of normalised kinetic rate constants of the second regime with mean linear flow velocity for Cu ($I = 0.27$ A) and Ag ($I = 0.5$ A).

$$\ln\left(\frac{C}{C_o}\right) = -k_m A_e \left(\frac{V_e}{V}\right) t \quad (4)$$

k_m being a characteristic mass transfer coefficient. Comparing Eqs. (2) and (4) then allows to conclude that

$$k_2 = k_m A_e \frac{V_e}{V} \quad (5)$$

Moreover, when considering a linearised diffusion equation at the surface of the electrode, it is easily shown [3] that k_m can be expressed as follows:

$$k_m = \frac{D}{\delta} \quad (6)$$

with D the diffusion coefficient and δ the thickness of the diffusional boundary layer. From the concentration data represented in Fig. 2 and fitted according to Eq. (4), we can therefore calculate a value for k_mA_e. At $v = 7 \times 10^{-2}$ m/s, this results in $k_mA_e = 1.49 \pm 0.02\ s^{-1}$ for Ag and $k_mA_e = 0.50 \pm 0.02\ s^{-1}$ for Cu. Further assuming a constant A_e value of 66 cm^2/cm^3, these k_mA_e data then correspond to a characteristic mass transfer coefficient $k_m = D/\delta$ of $(22.6 \pm 0.03) \times 10^{-3}$

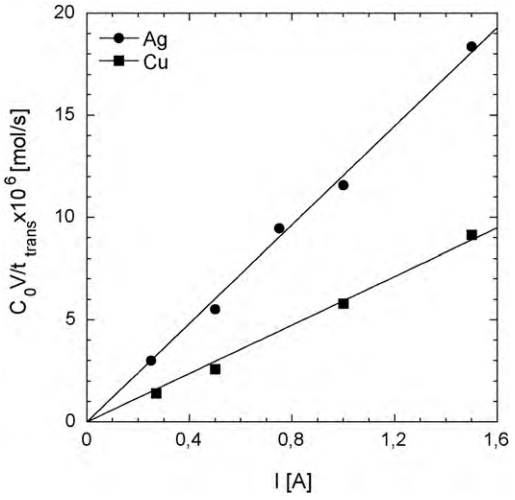

Fig. 6. Evolution of the inverse of the normalised transition time with applied current ($v = 7 \times 10^{-2}$ m/s).

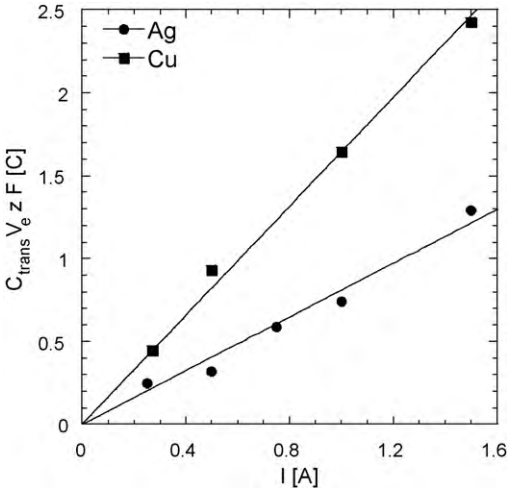

Fig. 7. Evolution of the normalised concentration at the transition with applied current ($v = 7 \times 10^{-2}$ m/s).

and $(7.6 \pm 0.3) \times 10^{-3}$ cm/s for Ag and Cu, respectively (always at a linear flow rate of 7×10^{-2} m/s). The different values obtained for Ag and Cu are mainly due to their different room temperature diffusion coefficient D, reported values being, respectively, 1.65×10^{-5} cm^2/s for Ag [9] and 0.49×10^{-5} cm^2/s for Cu [3]. The corresponding values for δ are then, respectively, 7.3 and 6.5 μm. Both the magnitude and similarity of these values is encouraging. We should nonetheless point out that the $k_m A_e$ value for Cu is about a factor 2 higher than the value of 0.23 s^{-1} mentioned in the literature [3] at similar flow rates. However, these experiments were carried out under potentiostatic control, with the overpotential being sufficiently small to avoid any parasitic hydrogen evolution. Under the galvanostatic conditions used in this work, the evolution of hydrogen bubbles is very likely in the second regime, so that the higher mass transport coefficient we obtained may arise from the enhancement of mass transfer by the generated gas bubbles, as recently suggested by Saleh [8]. Another possibility is that the concurrent hydrogen evolution reaction results in a dendritic deposit, as observed by Nikolic et al. [7], thereby increasing the specific surface area A_e of the electrode.

3.2. Kinetic transitions

Fig. 6 shows the evolution with applied current of the inverse of the transition time t_{trans}, normalised by the initial concentration and the catholyte volume. The transition time was determined as the intersection of the linear regression of the first regime and the logarithmic regression of the second regime. It is seen that this parameter varies linearly with applied current. This can be rationalised by first writing the differential equation for the reaction at the cathode–electrolyte interface in the first regime:

$$\frac{dC_i}{dt} = f\frac{dC}{dt} = -f\frac{I\eta}{zFV} \tag{7}$$

with C_i the metal ion concentration at the cathode surface, which we assumed here to vary linearly with the bulk concentration ($C_i = fC - m$), consistent with the assumption of a linear diffusion profile as shown by Walsh [10]. After integration, we obtain

$$C_i = C_{i,o} - \frac{f I\eta}{zFV} \quad t \tag{8}$$

with $C_{i,o}$ the initial metal ion concentration at the cathode surface, which we can reasonably assume to be equal to C_o. Rearranging Eq. (8) then finally results in

$$\frac{(C_o - C_{i,trans})V}{t_{trans}} = \frac{f I\eta}{zF} \tag{9}$$

$C_{i,trans}$ being the concentration at the cathode surface at $t = t_{trans}$. Fig. 6 indicates that, both in the case of Ag and Cu electrorecovery, the linear regressions pass through the origin. This implies that, based on Eq. (9), $C_{i,trans}$ is negligibly small relative to C_o or, in other words, that the kinetic transition for Ag and Cu electrorecovery occurs when their respective limiting currents have been reached. It is also seen from Eq. (9) that in that case, the slope of the linear regressions in Fig. 6 allow for another, independent calculation of the current efficiency. The thus obtained values for $f\eta$ are 1.17 ± 0.05 and 1.14 ± 0.04 for Ag and Cu, respectively, the ratio of which being similar to the ratio of η values obtained previously from the fit of the k_1 data in Fig. 3. Moreover, f being close to unity (so that $C_i \cong C - m$), this also implies that the slope of the linear diffusion profile during electrorecovery is quasi-independent of the bulk concentration, this slope being only dependant on the diffusion layer thickness and diffusion coefficient.

Finally, since it was concluded from Fig. 6 that the kinetic transition occurs when the limiting current I_{lim} is reached, we can expect, based on the definition of I_{lim} [3]:

$$I_{lim} = C_{trans} V_e z F k_m A_e \tag{10}$$

that the bulk concentration at the transition C_{trans} evolves itself also linearly with the applied current. Fig. 7 shows that this is indeed the case, both for Ag and Cu electrorecovery. Eq. (10) then allows for another independent calculation of the value of $k_m A_e$ from the slopes of the linear fit in Fig. 7. This gives a value of 1.23 ± 0.04 and 0.61 ± 0.01 s^{-1} for Ag and Cu, respectively, very close to the values previsously obtained from Eq. (4).

3.3. Electrode morphology

The SEM micrographs of Fig. 8 show the morphologies of the Cu deposit, both in the first (a) and second (b and c) kinetic regime (pictures b and c correspond to experiments with two different applied currents). While the deposit in the first regime appears relatively uniform, significant roughening takes place in the second regime, leading at lower current (b) to dendritic-like deposits. Characteristic morphologies of the Ag deposit are shown in Fig. 9 for the first (a) and the second (b) regime. In this case, a three-dimensional structure already appears in the first regime. The micrographs shown in

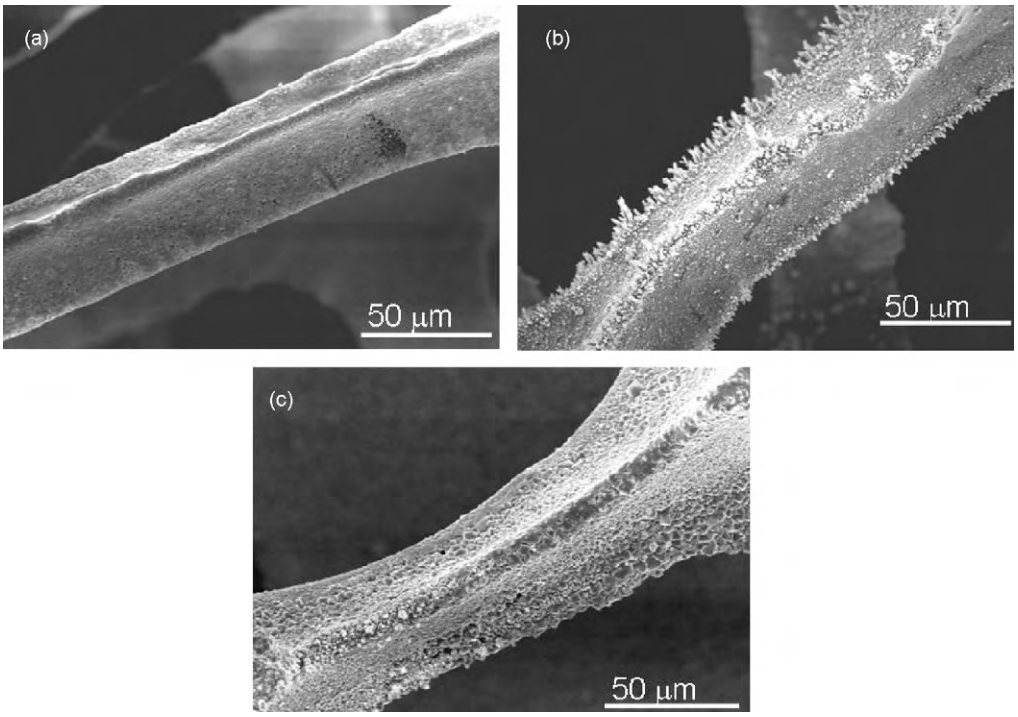

Fig. 8. SEM micrographs of Cu-covered RVC taken at (a) 0.65 A after 5 min, (b) at 0.65 A after 90 min and (c) at 1 A after 30 min ($v = 4 \times 10^{-2}$ m/s).

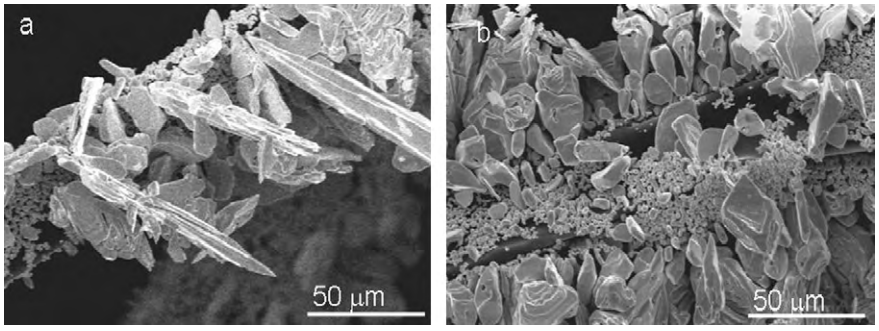

Fig. 9. SEM micrographs of Ag-covered RVC taken at 1 A: (a) after 8 min and (b) after 22 min ($v = 7 \times 10^{-2}$ m/s).

Figs. 8 and 9 therefore do not allow to make any conclusive statements on how each kinetic regime affects the final morphology of the deposit.

4. Conclusions

- RVC cathodes were used in a filter press cell to remove copper an silver ions from a sulphate solutions under galvanostatic conditions at different flow rates.
- Two kinetic regimes were observed, the first being electron-transfer limited and the second one being mass transfer limited.
- Based on the kinetic rate constants, the current efficiency in the first regime was calculated to be 0.88 ± 0.01 and 1.03 ± 0.03 for Cu and Ag, respectively. The relevant mass transport coefficient $k_m A_e$ amounts to, respectively, $0.50 \pm 0.02\ s^{-1}$ for Cu and $1.49 \pm 0.02\ s^{-1}$ for Ag at a linear flow rate of 7×10^{-2} m/s.
- Analysis of the time and concentration at the kinetic transition was shown to allow for an additional, independent calculation of both the current efficiency and mass transport coefficient, and to confirm that the kinetic transitions occur when the limiting current has been reached.
- SEM micrographs did not provide any conclusive evidence as to how each kinetic regime affects the morphology of the deposit.

References

[1] J. Wang, Electrochimica Acta 26 (1981) 1721–1726.
[2] I.C. Agarwal, A.M. Rochon, H.D. Gesser, A.B. Sparling, Water Research 18 (1984) 227–232.
[3] D. Pletcher, I. Whyte, F.C. Walsh, J.P. Millington, Journal of Applied Electrochemistry 21 (1991) 659–666.
[4] D. Pletcher, I. Whyte, F.C. Walsh, J.P. Millington, Journal of Applied Electrochemistry 21 (1991) 667–671.
[5] D. Pletcher, I. Whyte, F.C. Walsh, J.P. Millington, Journal of Applied Electrochemistry 23 (1993) 82–85.
[6] G.W. Reade, A.H. Nahle, P. Bond, J.M. Friedrich, F.C. Walsh, Journal of Chemical Technology and Biotechnology 79 (2004) 935–945.
[7] N.D. Nikolic, L.J. Pavjovic, M.G. Pavlovic, K.I. Popova, Electrochimica Acta 52 (2007) 8096–8104.
[8] M. Saleh, Journal of Solid State Electrochemistry 13 (2009) 343–351.
[9] CRC Handbook of Chemistry, David R. Lide, 2002–2003, pp. 5–95.
[10] F.C. Walsh, Transactions of the Institute of Metal Finishing 70 (2) (1992) 95–99.